RSC Advances

PAPER

View Article Online
View Journal | View Issue

Cite this: *RSC Adv.*, 2020, **10**, 39693

Effects of synthesised polyaniline (PAni) contents on the anti-static properties of PAni-based polylactic acid (PLA) films

Pei-Yi Wong, [a] Sook-Wai Phang *[b] and Azizah Baharum *[ac]

An anti-static polymer film was prepared using biodegradable poly(lactic acid) as a matrix and polyaniline (PAni) as an anti-static agent. It is aimed to be applied in packaging applications to dissipate the accumulated charges. The anti-static properties of PLA films were investigated with various PAni contents ranging from 0% to 20% through *ex situ* polymerisation by the solution casting method. PAni was synthesised in the solution form through chemical oxidation at 0 °C. The synthesis of PAni was confirmed by Fourier transform infrared (FTIR) spectroscopy and ultraviolet-visible (UV-Vis) absorption spectroscopy. The mechanical and anti-static properties of the samples were characterised using a Universal Testing Machine (UTM) and a resistivity meter, respectively. The experimental results indicated that incorporation of PAni into PLA films affected the morphology, anti-static and mechanical properties of the samples. PLA/PAni showed a compact surface with a porous structure, reflecting the interfacial interaction between PLA and PAni in the presence of a plasticiser. It was discovered and compared with other compositions, PLA with 15% PAni exhibited excellent anti-static performance with 2.45×10^{10} ohm/sq surface resistivity and the highest tensile strength, elongation at break and modulus of 29.3 ± 2.4 MPa, 60.1 ± 1.6% and 1364.0 ± 85.2 MPa respectively. Hence, PAni is a good candidate to be used in PLA/PAni systems by giving a suitable surface resistivity that can potentially be applied in anti-static packaging applications.

Received 17th August 2020
Accepted 15th October 2020

DOI: 10.1039/d0ra07076a

rsc.li/rsc-advances

Introduction

Packaging is widely used in daily life to protect the products during distribution, storage, sale, and transportation. In fact, plastic packaging is designed for the purposes and available in various colours, shapes, and sizes. The ease in manufacturing, chemical stability, and hygiene increase the usage of plastic packaging. Examples of commodity synthetic polymers used for packaging application are polyethene (PE), polypropylene (PP), polyvinyl chloride (PVC) and polystyrene (PS).[1] However, those synthetic polymers do not decompose easily under a normal environmental condition and have a significant impact on the environment. Much terribly when a large accumulation of used synthetic polymers enters into the ocean tend to threaten the marine lives. Similarly, pollution issues raise dramatically when the population size increases and quality waste management systems are lacking.[2] Therefore, bio-based plastic plays an essential role in replacing the usage of conventional plastic packaging.[3]

Recently, various types of bio-based plastics such as polyamide 11, polylactic acid (PLA) and polyhydroxyalkanoates (PHA) have been introduced. Among all, PLA gains the most interest among the researchers, which is owing to its unique features. For instance, PLA can be synthesised from renewable resources, the processability is easy and it is biodegradable.[4,5] Synthesised packaging based on PLA can be fully degraded into carbon dioxide and water under certain conditions.[6] This biodegradable behaviour can reduce the environmental pollution caused by the conventional plastic packaging. Despite the fact that PLA is a bio-based plastic, PLA behaves as a non-conductive polymer and tends to trigger electronic discharge (ESD) events when it is applied in packaging.[7] Thus, the modification and development of packaging based on PLA that inherited an anti-static property required to avoid ESD events.

Generally, conventional plastic packaging applied anti-static agents such as carbon black, graphene, silver, and copper powder to inherit the anti-static properties in order to prevent ESD events.[8] The anti-static agents created a thin conductive layer on the surface of packaging to eliminate the static charges trapped. Nonetheless, short-term performance, low

[a]*Department of Chemical Sciences, Faculty of Science and Technology, Universiti Kebangsaan Malaysia, 43600 Bangi, Selangor, Malaysia. E-mail: wyyerwong@gmail.com*

[b]*Department of Physical Science, Faculty of Applied Sciences, Tunku Abdul Rahman University College, Jalan Genting Klang, 53300 Kuala Lumpur, Malaysia. E-mail: pinkyphang@gmail.com*

[c]*Polymer Research Center, Faculty of Science and Technology, Universiti Kebangsaan Malaysia, 43600 Bangi, Selangor, Malaysia. E-mail: azeiss@ukm.edu.my*

transparency and high toxicity are some of the drawbacks of the currently used anti-static agents.

The perception of the polymer is an insulator that has been changed due to the discovery of conducting polymers (CPs). Examples of the common CPs are polythiophene (PTh), polypyrrole (PPy) and polyaniline (PAni).[9] The conjugated double bond of the CP enables the "jumping" action of the electrons along the backbone and exhibits high electrical conductivity.[10] The CP is useful in a wide range of applications such as electronic devices, diodes, chemical sensor, catalysts for fuel cells and supercapacitors.[11,12] Among all CPs, PAni is one of the favourite CP studied by researchers due to low processing cost and sustainability as compared to others.[13,14] Furthermore, PAni can exist in different oxidation states with different colours and structures that inspired researchers to investigate it further.[15]

In this research work, PAni was used, which acted as an anti-static agent in the PLA film. It is a combination of biodegradable polymer and CP to characterise the properties of polymer films for packaging application. PAni was synthesised by a chemical oxidation method. Then, PLA/PAni was prepared with different contents of PAni (0–20%) by a solution casting method. The functional group, conducting behaviour, mechanical properties and surface morphology of the polymer films were analysed by Fourier transform infrared (FTIR) spectroscopy, ultraviolet-visible (UV-Vis) spectroscopy, tests using a Universal Testing Machine (UTM) and scanning electron microscopy (SEM), respectively. The anti-static properties of the polymer films were monitored by observing the resistivity by a four-point probe method.

Experimental

Materials and chemicals

All the chemicals used in the synthesis of PAni such as aniline (Ani) (99%) monomers, ammonium persulfate (APS) (98%) oxidants, and dioctyl sodium sulfosuccinate (AOT) dopants (96%) were purchased from Sigma Aldrich, USA. Meanwhile, toluene (99.5%) that acted as the solvent to extract the PAni precipitates was purchased from Chemiz, Malaysia. Hydrochloric acid (37%) dopant used was provided by R&M Chemicals, Malaysia. Tetrahydrofuran (THF) (99.8%) used as the medium to dissolve PLA was provided by R&M Chemicals, Malaysia. Glycerol (Gly) (99.5%) of analytical grade was purchased from Friendemann Schmidt, USA. PLA resin (semi-crystalline form) was purchased from NatureWorks® PLA, 2003D, USA, with a melt flow index of 6.0 g/10 min at a temperature of 210 °C and a specific gravity of 1.24. All chemicals were used without further purification. Distilled water was obtained and purified by simple distillation.

Synthesis of PAni

In this study, PAni was synthesised using an Ani : AOT monomer in the ratio of 5 : 5 by a chemical oxidation method. Firstly, AOT was dissolved in 1 M HCl. Then, Ani was added drop by drop into the AOT solution and stirred vigorously using a magnetic stirrer. After that, the APS solution was added slowly to the solution mixture. The polymerisation was carried out at 0 °C for 24 hours. Once the polymerisation was done, toluene was added into the solution mixture to extract the PAni precipitates formed. The PAni solution was washed three times with distilled water to remove the non-reacted APS, AOT and Ani monomer respectively. Finally, the percentage of PAni in the toluene solution was determined.[16]

Synthesis of PLA/PAni films

PLA/PAni films were prepared with different contents of PAni: 0% to 20% by a solution casting method. First, PLA resin was pre-heated in a conventional oven at 50 °C for 24 hours to remove the moisture content. Then, PLA (~6.0 g) was dissolved in 100 mL of THF (100 mL) solution with continuous stirring at 60 °C. The glycerol (1.8 g) acting as a plasticiser was added into the dissolved PLA solution. After that, synthesised PAni was then slowly added into the PLA solution. The mixed solution was stirred at 60 °C for 24 hours. The mixtures were cast onto a glass dish (diameter 150 mm, height 15 mm) and dried at room temperature overnight. The dried PLA/PAni films were kept in sealed polyethene bags and stored in desiccators at room temperature before further characterisation. In this study, glycerol acts as a plasticiser to form a connection bridge and link PLA and PAni to obtain a better and smooth film. The resulted sample could not form a film for the formulation of PLA/PAni without the addition of glycerol.

Characterisation techniques

The chemical structure of PAni was determined using a Shimadzu Model IRTracer-100 Fourier transmission infrared (FTIR) instrument with Attenuated Total Reflection (ATR) mode from Shimadzu Scientific Instruments (SSI), Japan. FTIR spectroscopy was used to identify the functional group of PAni in the wavenumber range of 400 cm^{-1} to 4000 cm^{-1} at room temperature. UV-Vis spectra of PAni were recorded using a Hitachi Ultraviolet-Visible (UV-Vis) Spectrophotometer Model U-2900 from Hitachi, Japan. The measurement range of the UV-Vis wavelength was from 300 nm to 900 nm to determine the oxidation states of synthesised PAni.

The anti-static properties of PAni/PLA films were monitored by observing the surface resistivity of the film. The surface resistivity of PLA/PAni films was measured using a resistivity meter (Hiresta MCP-HT800, from Mitsubishi Chemical Analytech, Japan) at room temperature by a four-point probe method. The measurement ranges of surface resistivity for this instrument was from 10^5 to 10^{12} ohm/sq. The surface morphology of pristine PLA and PLA/PAni films was observed using a scanning electron microscope (SEM) Merlin Compact (MERLIN-6025, from Carl Zeiss, UK) at both magnifications of 500× and 20 000× at an accelerating voltage of 3.0 kV. The polymer films were placed on the aluminium stubs and coated with iridium to make the polymer films to be conductive before SEM analysis. Meanwhile, the cross-section of the polymer films was cut and coated with iridium before SEM analysis.

Furthermore, the mechanical properties of the PAni/PLA films were studied from the tensile strength, elongation at

break and tensile modulus of the films. The mechanical test was performed using a Universal Testing Machine (UTM) from Jinan Testing Equipment IE Corporation, China, equipped with a load cell of 1 N and the UTM 107 software. The polymer films were cut into dumbbell-shaped specimens and the mechanical test was conducted at a temperature of 23± 2 °C and relative humidity (RH) of 50 ± 5%. The mechanical properties of the PLA/PAni films were characterised according to the ASTM D638 standard. The initial gauge separation and crosshead speed were set as 15 mm and 0.5 mm/s respectively. The tensile strength, elongation at break and tensile modulus of the polymer films were recorded accordingly at room temperature.

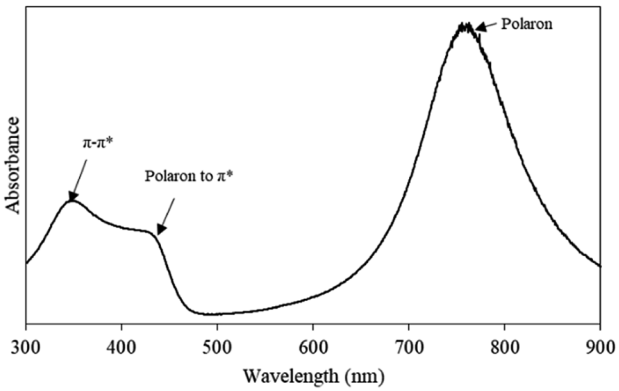

Fig. 2 UV-Vis spectrum of synthesised PAni.

Results and discussion

Fig. 1 shows the FTIR spectra of pristine PLA, pristine PAni and PLA/PAni (PAni 15%) films. PLA and PAni samples without the addition of glycerol were unable to form a film, and hence, the performance of PLA casting with PAni without glycerol as a control sample could not be reported. For pristine PLA, the absorption band ranging from 3250 cm^{-1} to 3571 cm^{-1} attributed to the O–H stretching vibration of pristine PLA was recorded. The absorption band at 1746 cm^{-1} was assigned to the C=O stretching vibration of pristine PLA. The absorption bands situated at 1447 cm^{-1} and 1359 cm^{-1} were assigned to the deformation vibration of C–H from PLA.[17]

For pristine PAni, the N–H stretching vibration of PAni was located at 3215 cm^{-1} while the quinoid and benzenoid rings of the PAni were observed at the peak of 1584 cm^{-1} and 1487 cm^{-1}, respectively.[16] Meanwhile, C–N stretching can be found at the peak of 1244 cm^{-1}, which indicates that PAni was highly doped and presented in emeraldine salt (ES) states.[18] The band observed at 803 cm^{-1} were ascribed to the bending vibration of the C–H bond in the *para*-disubstituted rings of PAni.

Generally, all PLA/PAni films (PAni 5–20%) possessed similar FTIR spectrum patterns from 400 cm^{-1} to 4000 cm^{-1}. The FTIR spectrum of PLA/PAni (PAni at 15%) exhibited both characteristic peaks of pristine PLA and pristine PAni. By comparing the FTIR spectra in Fig. 1, it can be observed that the characteristics peaks of the PLA/PAni film were shifted slightly to a higher wavenumber than that of pristine PLA and pristine PAni. This could be due to the presence of water during the preparation of PLA/PAni films, which affects the amount of H^+ related to the oxidant in the reaction medium. Thus, the reversible oxidation states of PAni were slightly affected and resulted in the wavenumber shift for PLA/PAni films.[19]

The position of the ester group and the C=O stretching vibration of PLA did not change but appeared as a sharper peak at 1752 cm^{-1}. This reflected the ester linkage of O–H from glycerol between PLA and PAni. Besides, the quinoid and benzenoid rings of PAni were observed at 1457 cm^{-1} and 1354 cm^{-1} in the PLA/PAni film similar to pristine PAni.[20] However, the broad peaks ranging from 3200 cm^{-1} to 3500 cm^{-1} in PLA/PAni reflected the mutual interaction between N–H of PAni and O–H of PLA. Thus, the N–H peak disappeared in the PLA/PAni spectrum due to the interaction between PAni and PLA.[21] This result also consolidates the assumption that PLA/PAni was compatible. The C–H stretching vibration remains unchanged at the same position at 865 cm^{-1}, 855 cm^{-1} and 871 cm^{-1} for the PLA, PAni and PLA/PAni films respectively.

Fig. 2 shows the UV-Vis absorption spectrum of pristine PAni ranging from 300–900 nm. There are three characteristic peaks observed in the UV-Vis spectrum, including ~350 nm,

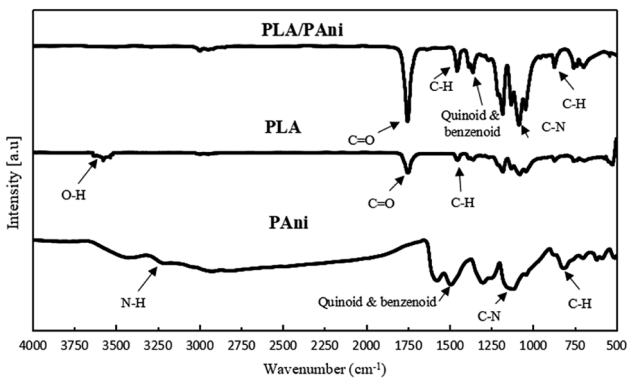

Fig. 1 FTIR spectra of pristine PLA, pristine PAni and PLA/PAni (PAni 15%) films.

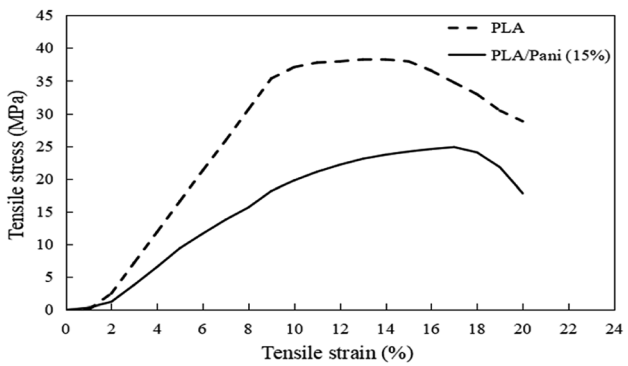

Fig. 3 Stress–strain curves of PLA and PLA/PAni films at 15% of PAni loading.

Table 1 Mechanical properties obtained by the tensile test for PLA (0%) and PLA/PAni (5–20%) films

Samples	Tensile strength (MPa)	Elongation at break (%)	Tensile modulus
PLA (0%)	38.2 ± 2.2	17.1 ± 3.0	808.6 ± 123.4
PLA/PAni (5%)	17.3 ± 1.2	25.8 ± 2.2	618.4 ± 88.6
PLA/PAni (10%)	25.1 ± 1.5	41.7 ± 3.6	788.0 ± 47.4
PLA/PAni (15%)	29.3 ± 2.4	60.1 ± 1.6	1364.0 ± 85.2
PLA/PAni (20%)	22.5 ± 2.2	25.9 ± 1.5	856.7 ± 71.5

~430 nm, and ~770 nm. The absorption peak at ~350 nm corresponded to the π–π* transition of benzenoid rings, while the absorption peak at ~430 nm, indicated the polaron-to-π* transition and localised polaron of protonated imines C=N of PAni.[22] Meanwhile, the absorption peak at ~770 nm referred to the ES conductive states of PAni. Therefore, FTIR and UV-Vis spectra significantly confirmed the chemical structure of PAni in ES conductive states.

Generally, PLA with different contents of PAni showed a similar pattern of stress–strain curves. Thus, Fig. 3 shows the stress–strain curves for PLA without and with the addition of 15% PAni loading only. Meanwhile, tensile strength, elongation at break and tensile modulus for all samples were extracted from stress–strain curves, and they are tabulated in Table 1. Fig. 4 shows the tensile strength, elongation at break and modulus of the PLA blend with different PAni loadings (0–20%), respectively. From Fig. 4, it can be noted that the tensile strength of the polymer blend significantly reduced with the addition of PAni from 38.2 ± 2.2 MPa (pristine PLA) to 17.3 ± 1.2 MPa to 29.3 ± 2.4 MPa (PLA/PAni). Principally, PLA is well known as highly orientated with a long branched-chain polymer. PLA used in this study presented in a semi-crystalline form that possesses high tensile strength (38.2 ± 2.2 MPa). After the addition of PAni into the PLA blend, the crystalline region of the polymer chain in PLA was disrupted. This eventually reduced the degree of crystallinity of the polymer and induced more free volume among the matrix. As a result, the tensile strength of the polymer blend (17.3 ± 1.2 MPa to 29.3 ± 2.4 MPa) decreased.[23]

In Fig. 4, the tensile strength and tensile modulus display a similar trend, indicating that 15% of PAni loading is the optimum percentage for the blend. The tensile strength of the polymer blend increased gradually from 17.3 ± 1.2 MPa to 29.3 ± 2.4 MPa, while the tensile modulus of the polymer blend increased significantly from 618.4 ± 88.6 MPa to 1364.0 ± 85.2 MPa with the increase in PAni loading from 5% to 15%. This could be due to the plasticisation effect of glycerol in PLA/PAni films.[24] During the preparation of polymer blends, glycerol was added into the system as a plasticiser to decrease the plasticity of PLA/PAni films and produce homogeneous and smooth films. Glycerol tends to convert the rigid structure of PLA/PAni into a soft, flexible and elastic material that possesses higher tensile strength.[25] This explanation was supported by Liu and his co-workers researching on the effect of glycerol and water on the properties of PLA blends.[26,27] Furthermore, the stiffness of PLA/PAni films also improved due to the PAni backbone, which restricted the chain mobility of the PLA matrix, thereby improving the tensile modulus of the polymer blend.[28]

Oppositely, the elongation at break of the polymer blend with the addition of PAni does not show a similar trend as tensile strength and tensile modulus. Generally, the PLA/PAni film possesses a higher percentage of elongation at break as compared to the pristine PLA film. The elongation at break of the polymer blend increased significantly from 17. ± 3.0% to 60. ± 1.6% with the increase in PAni loading from 0% to 15%. This could be due to the increase in PAni loading that restricted the molecular mobility of PLA chains and eventually improved the resistance of plastic deformation.[24,29,30] Therefore, the PLA/PAni film showed tougher properties than the pristine PLA film by giving higher elongation at break values.

However, the addition of a huge amount of PAni (>15%) to PLA/PAni films led to the aggregation of PAni and made the PLA/PAni system heterogeneous.[31,32] Thus, it eventually reduced the tensile strength, elongation at break and tensile modulus of the polymer blend. The explanation was supported by Ghani and co-workers (2015) who prepared poly(vinyl chloride)/

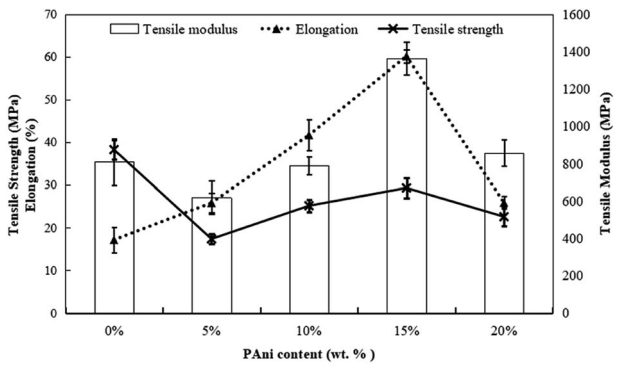

Fig. 4 Effect of PAni contents on the tensile modulus, tensile strength and elongation at break of PLA/PAni films.

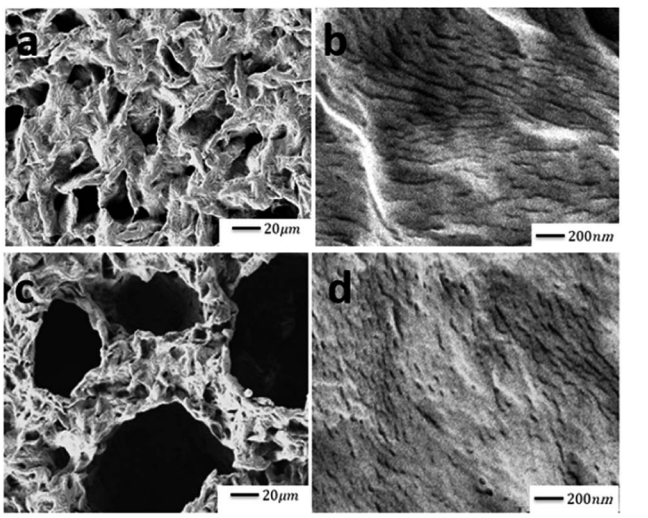

Fig. 5 SEM images of (a) PLA at 500×, (b) PLA at 20 000×, (c) PLA/PAni films with 15% PAni loading at 500× and (d) PLA/PAni films with 15% PAni loading at 20 000×.

poly(ethylene oxide) blend films with the addition of PAni.[33] Therefore, the optimum percentage of PAni loading for the PLA/PAni film was 15% by showing the highest tensile strength, elongation at break and modulus of 29.3 ± 2.4 MPa, 60. ± 1.6% and 1364.0 ± 85.2 MPa, respectively.

Fig. 5 shows the morphology of PLA and PLA/PAni films with the magnification of 500× and 20 000×, respectively. Referring to Fig. 5(a) and (b), the PLA matrix showed a rough and loosened surface as similar to Ibrahim *et al.* (2013) reporting the effect of the treated *Typha latifolia* on PLA.[34] Furthermore, the PLA/PAni film with 15% PAni loading produced smooth and compact surfaces, as observed in Fig. 5(c) and (d). The smooth and dense surfaces of PLA/PAni revealed a good dispersion of PAni into the PLA matrix. The good dispersion was attributed to good interfacial interaction between PLA and PAni. This result shows good agreement with the finding as reported by Shahdan and his co-worker (2018), which investigated the properties of PLA and modified natural rubber blends with a low loading of PAni.[41]

By comparing pristine PLA and PLA/PAni films, the porous diameter of PLA significantly increased from 4.4 μm to 27.25 μm for PLA/PAni based on the SEM morphology. The porosity increment of the system was also presented identically by Azlinnorazia and co-workers.[35] This increment in porosity can be explained by the proposed mechanisms, as shown in Scheme 1.

In this study (referring to Scheme 1), glycerol is added into the polymer blend as a plasticiser to link both the PAni and PLA through chemical interaction. The ester bond of PLA backbone tends to crosslink covalently to the glycerol and form a three-dimensional network of random coils when interacting with PAni.[36,37] The mechanism in Scheme 1 was supported by the glycerol and sebacic acid research work done by Wang and co-workers.[38] Nonetheless, the hydrophilic character of glycerol with –OH group tends to repel each other in the polymer matrix due to the hydrophilic repulsion between the PAni and PLA. Thus, this resulted in low crosslink density and formed a compact structure of PLA/PAni with higher porosity, as shown in Fig. 5.[39] The proposed mechanism in this study was also supported by the research work about glycerol-based biopolyesters done by Valerio and co-workers in 2016.[40]

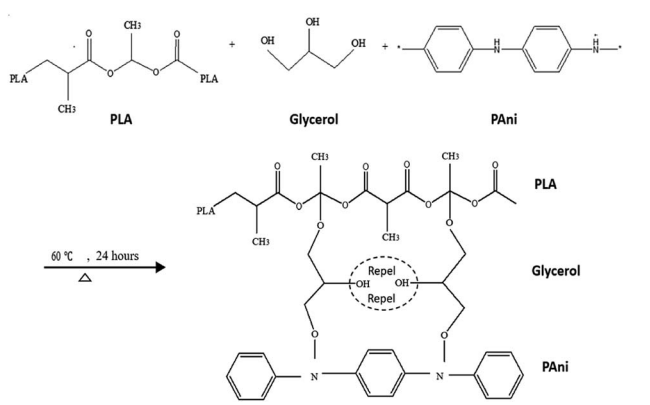

Scheme 1 Mechanisms of PLA and PAni with the addition of glycerol.

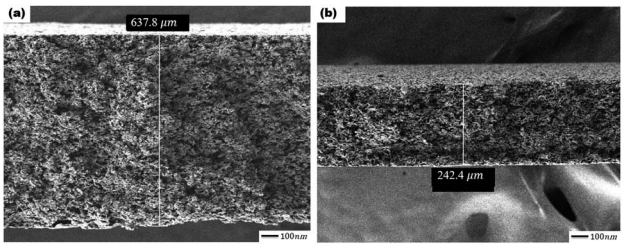

Fig. 6 SEM images for cross-section of (a) PLA at 100× and (b) PLA/PAni films at 15% of PAni loading at 100×.

Fig. 6 shows the cross-section images of pristine PLA and PLA/PAni (15%) films using an SEM instrument with a magnification of 100×. Based on Fig. 6, the pristine PLA film was thinner and firmer with a thickness of 242.4 μm. After the addition of PAni into PLA, the PLA/PAni film formed a thicker film with higher porosity with a thickness of 637.8 μm. The thickness of PLA/PAni film increases as compared to the pristine PLA film, which could be due to the interface properties of the PLA and PAni. This phenomenon can be explained by the phase segregation in the PLA/PAni film that occurred and leads to micro-layered separation.[24]

Fig. 7 shows the surface resistivity of PLA/PAni with the different contents of PAni ranging from 0% to 20%. The surface resistivity of the polymer blend decreased gradually from 1.25×10^{12} ohm/sq (pristine PLA) to 4.26×10^{8} to 8.37×10^{11} ohm/sq (PLA/PAni) after the addition of PAni. The anti-static properties of the PLA/PAni films were evaluated by the surface resistivity of the films. Based on the ESD Association Standard, the surface resistivity of the materials falls from the range of 10^{9} to 10^{12} ohm/sq were considered as good anti-static materials. Meanwhile, the surface resistivity of the materials showed in the range of 10^{11} to 10^{12} ohm/sq revealed the materials only provided sufficient anti-static effort. Consequently, a material with a surface resistivity higher than 10^{12} ohm/sq is known as a non-anti-static material or an insulating material.[42] Thus, PLA/PAni films produced in this research with a surface resistivity in the range of 4.26×10^{8} to 8.37×10^{11} ohm/sq were considered as good anti-static materials.

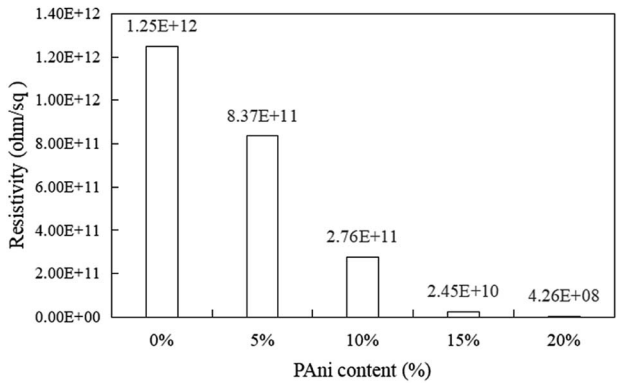

Fig. 7 Electrical conductivities of PLA/PAni films with different PAni contents.

Based on Fig. 7, pristine PLA possessed the highest surface resistivity of 1.25×10^{12} ohm/sq because pristine PLA is known as an insulating film. The unavailability of free electrons in the pristine PLA made the electrons unable to drift along the polymer backbone. Therefore, this resulted that pristine PLA was an insulating material. Meanwhile, the surface resistivity of the PLA/PAni film significantly reduced after the addition of PAni into the polymer blend. This is because PAni is a conjugated polymer that can create the conductive pathway along the PAni chain inside the polymer blend. The delocalised electrons from the doped PAni propagated along the polymer chain and inherited the polymer blend with high conductivity.[43] Consequently, the addition of PAni increased the conductivity by showing low surface resistivity and exhibited good anti-static properties in the PLA/PAni films.

The proposed illustration of the accumulated static charges toward the surface of the PLA/PAni film is shown in Fig. 8. The conductive layer of PAni acted as the anti-static agent and bound to the PLA matrix with the aid of glycerol. In general, accumulated static charges were generated by the triboelectric effect or physical friction contact surrounded the films.[44] As a result, the anti-static PAni consists of polar and non-polar surfaces, as shown in Fig. 8. The polar and non-polar surfaces of the PAni layer will interact with each other to reduce and eliminate the build-up of static charges on the surfaces and increase the safety for application.

Furthermore, the surface resistivity of PLA/PAni significantly decreased with increasing in PAni contents. According to Ohms' law, the conductivity of a polymer is the reciprocal of the resistivity, where the resistivity is known as the resistance to the flow of the electric current. Thus, the higher the conductivity with increasing PAni contents, the lower the surface resistivity of the polymer blends. As PAni contents increased, the conductive path and delocalised electrons from the doped PAni eventually increased, resulting in higher propagation of electrons along the polymer chain. Therefore, the surface resistivity of the PLA/PAni film decreased.

However, the PLA/PAni film with the addition of the PAni in the range of 5–15% possessed anti-static properties as the surface resistivity fall in the range of 10^9 to 10^{12} ohm/sq according to the standard anti-static range based on the ESD Association Standard as mentioned earlier. As a result, PLA/PAni with 5–15% PAni loading is suitable to be used for static charge protection in packaging films.[42] Although PLA/PAni films with 20% of PAni loading showed the lowest surface resistivity of 4.26×10^8 ohm/sq, it is not recommended to be used for anti-static application as the surface resistivity was out of the suggested standard anti-static range.

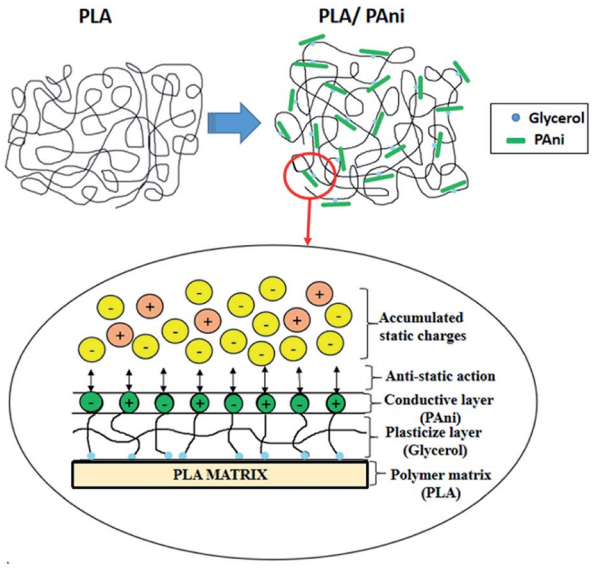

Fig. 8 Proposed illustration of the accumulated static charges toward the PLA/PAni film.

Conclusions

PAni has been successfully synthesised and applied as an anti-static agent in PLA/PAni films for packaging. The chemical structure of PAni was confirmed by FTIR and UV-Vis spectra. The synthesised PAni in this research showed ES states and possessed high electrical conductivity. From the SEM images, the compact and smooth structure of PLA/PAni significantly showed the chemical interaction between PAni and PLA in the presence of glycerol. The optimum percentage of PAni (15%) exhibited excellent mechanical properties of PLA/PAni films with tensile strength, elongation at break and modulus of 29.3 ± 2.4 MPa, 60.1 ± 1.6% and 1364.0 ± 85.2 respectively. PLA/PAni films produced in this research with surface resistivity in the range of 4.26×10^8 to 8.37×10^{11} ohm/sq were considered as good anti-static materials. In conclusion, this research eventually showed that conductive PAni could be used as an alternative material to replace the traditional anti-static agent, which is highly toxic (carbon black) and costly (TiO_2) for anti-static packaging.

Conflicts of interest

The authors declare no conflicts of interest associates with this work.

Acknowledgements

This research work was supported by the Research University (RU) grant coded as GUP-2017-123. The authors would also like to thank the Department of Chemical Sciences, Faculty of Science and Technology, Universiti Kebangsaan Malaysia for the support.

References

1 Z. A. Boeva and V. G. Sergeyev, *Polym. Sci., Ser. C*, 2014, **56**, 144–153.
2 R. E. Marshall and K. Farahbakhsh, *Waste Manag.*, 2013, **33**, 988–1003.
3 B. P. Chang, A. K. Mohanty and M. Misra, *RSC Adv.*, 2020, **10**, 17955–17999.

4 R. Sengupta, S. Chakraborty, S. Bandyopadhyay, S. Dasgupta, R. Mukhopadhyay, K. Auddy and S. Deu, *Polym. Eng. Sci.*, 2007, **47**, 21–25.
5 N. A. Rosli, I. Ahmad, F. H. Anuar and I. Abdullah, *J. Cleaner Prod.*, 2018, **198**, 987–995.
6 M. Yu, Y. Zheng and J. Tian, *RSC Adv.*, 2020, **10**, 26298–26307.
7 E. Galikhanov, I. Lounev, A. Guzhova, Y. Gusev, M. Galikhanov and M. Vasilyeva, *AIP Conf. Proc.*, 2016, **1722**, 1–5.
8 P. C. Plants and A. Update, *Initiatives*, 2006, 165–192.
9 I. S. Zaine, Z. M. Zabidi, A. N. Alias and M. H. Jumali, *Adv. Mater. Res.*, 2013, **658**, 237–241.
10 J. Nowaczyk, K. Kadac, I. Tarach and E. Olewnik-Kruszkowska, *J. Mater. Sci.: Mater. Electron.*, 2017, **28**, 19071–19080.
11 L. N. Shubha, M. Kalpana and P. Madhusudana Rao, *Der Pharm. Lett.*, 2016, **8**, 214–219.
12 F. De Salas, I. Pardo, H. J. Salavagione, P. Aza, E. Amougi, J. Vind, A. T. Martínez and S. Camarero, *PLoS One*, 2016, **11**, 1–18.
13 T. S. Chew, R. Daik and M. A. A Hamid, *Polymers*, 2015, **7**, 1221–1231.
14 J. Park, X. Yang, D. Wickramasinghe, M. Sundhoro, N. Orbey, K. F. Chow and M. Yan, *RSC Adv.*, 2020, **10**, 26486–26493.
15 M. Mohammad, S. Kamarudin, N. H. Mohamed, N. Asim and K. Sopian, *3rd International Conference on Smart Material Research*, 2017, vol. 293, pp. 1–5.
16 K. P. Sambasevam, S. Mohamad and S. W. Phang, *Mater. Sci. Semicond. Process.*, 2015, **33**, 24–31.
17 W. Shen, G. Zhang, X. Ge, Y. Li and G. Fan, *R. Soc. Open Sci.*, 2018, **5**, 180134.
18 Y. S. Chiam, I. Z. Mohamad Ahad, S. Wadi Harun, S. N. Gan and S. W. Phang, *Synth. Met.*, 2016, **211**, 132–141.
19 W. Shao, R. Jamal, F. Xu, A. Ubul and T. Abdiryim, *Materials*, 2012, **5**, 1811–1825.
20 X. Wang, Y. Tang, X. Zhu, Y. Zhou and X. Hong, *Int. J. Biol. Macromol.*, 2020, **146**, 1069–1075.
21 M. Panigrahi, S. B. Majumdar and B. Adhikari, *International Conference on Nanoscience, Technology and Societal Implications*, Bhubaneswar, 2011, pp. 1–7.
22 D. Y. Godovsky, A. E. Varfolomeev, D. F. Zaretsky, R. L. Nayana Chandrakanthi, A. Kündig, C. Weder and W. Caseri, *J. Mater. Chem.*, 2001, **11**, 2465–2469.
23 T. Takayama, K. Uchiumi, H. Ito, T. Kawai and M. Todo, *Adv. Compos. Mater.*, 2013, **22**, 327–337.
24 P. H. S. Picciani, E. S. Medeiros, Z. Pan, D. F. Wood, W. J. Orts, L. H. C. Mattoso and B. G. Soares, *Macromol. Mater. Eng.*, 2010, **295**, 618–627.
25 H. Yun, M. K. Kim, H. W. Kwak, J. Y. Lee, M. H. Kim and K. H. Lee, *Int. J. Biol. Macromol.*, 2016, **82**, 945–951.
26 J. Zhang, B. Liu, L. Jiang, H. Liu and L. Sun, *Macromol. Mater. Eng.*, 2010, **295**, 123–129.
27 K. Chantawee and S. A. Riyajan, *J. Polym. Environ.*, 2019, **27**, 50–60.
28 J. Bhadra, N. J. Al-Thani, N. K. Madi and M. A. Al-Maadeed, *Arabian J. Chem.*, 2017, **10**, 664–672.
29 T. Ceregatti, P. Pecharki, W. M. Pachekoski, D. Becker and C. Dalmolin, *Rev. Mater.*, 2017, **22**, 11863.
30 S. Kamthai and R. Magaraphan, *AIP Conf. Proc.*, 2015, **1664**, 06006.
31 H. Yu, C. Wang, J. Zhang, H. Li, S. Liu, Y. Ran and H. Xia, *Mater. Chem. Phys.*, 2012, **133**, 459–464.
32 N. P. S. Chauhan, K. Meghwal, M. Gholipourmalekabadi and M. Mozafari, *Polyaniline Blends, Composites, and Nanocomposites*, Elsevier, 2018, ch. 6, pp. 149–174.
33 S. A. Ghani, S. H. Mohd Din and J. Abd Jalil, *J. Vinyl Addit. Technol.*, 2018, **24**, 44–49.
34 M. Ibrahim, J. A. Jalil, S. N. S. Mahamud, Y. M. Daud, S. Husseinsyah and M. R. Yahya, *Key Eng. Mater.*, 2014, **594**, 775–779.
35 A. Ahmad, M. Z. Yunos, Z. Harun, M. F. Hassan, S. Adzila, A. M. T. Arifin, M. N. A. Rahman and R. H. A. Haq, *Chem. Eng. Trans.*, 2017, **56**, 691–696.
36 M. Frydrych, S. Román, S. Macneil and B. Chen, *Acta Biomater.*, 2015, **18**, 40–49.
37 S. M. Hikmatun Ni'mah, R. Rochmadi, E. M. Woo and D. A. Widiasih, *J. Chem. Inf. Model.*, 2019, **53**, 1689–1699.
38 Y. Wang, S. Lu, P. Gabriele and J. J. Harris, *Mater. Matters*, 2016, **11**, 3.
39 P. T. Bertuoli, J. Ordono, E. Armelin, S. Pérez-Amodio, A. F. Baldissera, C. A. Ferreira, J. Puiggalí, E. Engel, L. J. Del Valle and C. Alemán, *ACS Omega*, 2019, **4**, 3660–3672.
40 O. Valerio, J. M. Pin, M. Misra and A. K. Mohanty, *ACS Omega*, 2016, **1**, 1284–1295.
41 D. Shahdan, R. S. Chen, S. Ahmad, F. D. Zailan and A. Mat Ali, *Polym. Int.*, 2018, **67**, 1070–1080.
42 S. Chen, B. Zhou, M. Ma, Y. Shi and X. Wang, *Polym. Adv. Technol.*, 2018, **29**, 1788–1794.
43 T. H. Le, Y. Kim and H. Yoon, *Polymers*, 2017, **9**, 150.
44 M. Jafari, A. Rahimi, A. E. Shokrolahi and A. E. Langroudi, *J. Coat. Technol. Res.*, 2014, **11**, 587–593.